fishes

MDPI

Article

A Comparative Transcriptome Analysis Reveals the Effects of Letrozole and 17α-Methyltestosterone on the Expression of Reproductive-Related Genes in Golden Pompano (*Trachinotus ovatus*)

Qi Zhou [1,†], Yan Wang [1,†], Yuwen Guo [1], Guangli Li [1], Tao Wang [1,2,*] and Huapu Chen [1,2,*]

[1] Guangdong Research Center on Reproductive Control and Breeding Technology of Indigenous Valuable Fish Species, Guangdong Provincial Key Laboratory of Aquatic Animal Disease Control and Healthy Culture, Fisheries College, Guangdong Ocean University, Zhanjiang 524088, China
[2] Agro-Tech Extension Center of Guangdong Province, Guangzhou 510520, China
* Correspondence: wangtao01@gdou.edu.cn (T.W.); chenhp@gdou.edu.cn (H.C.)
† These authors contributed equally to this work.

Abstract: Aromatase inhibitor letrozole (LZ) and 17α-methyltestosterone (MT) are commonly used for sex control breeding to induce female-to-male sex reversal in aquaculture. However, studies on the molecular regulatory mechanisms of LZ and MT are still limited. Here, a comparative transcriptome analysis was conducted on the hypothalamus, the gonad, and the liver of golden pompano (*Trachinotus ovatus*) after 30 days of LZ and MT treatment, which demonstrated significant sexual size dimorphism. Following LZ treatment, the transcriptome data identified 156, 890, and 1286 different expression genes (DEGs) in the hypothalamus, the liver, and the gonad, respectively. After MT treatment, the transcriptome data identified 114, 876, and 950 DEGs in the hypothalamus, the liver, and the gonad, respectively. Functional enrichment analysis revealed that DEGs were involved in oocyte meiosis and steroid-hormone synthesis following LZ treatment. Similarly, the analysis indicated that DEGs were associated with cysteine and methionine metabolism and steroid-hormone synthesis after MT treatment. Further analysis showed that LZ treatment can promote the first meiotic division but inhibit the second meiotic division of the oocyte. MT treatment promotes polyamine synthesis to induce oocyte apoptosis, both of which affect the trajectory of ovarian differentiation in golden pompano. However, LZ and MT have converse effects in sex hormone synthesis. LZ inhibits estrogen metabolism but promotes cholesterol synthesis by regulating *sqle*, *cyp3a40*, *ugt1a1*, and *ugt2a1*, while MT promotes estrogen metabolism but inhibits the conversion of cholesterol to pregnenolone by regulating *cyp19a1*, *cyp1a*, and *hsd17b7*. This study reveals that both LZ and MT may inhibit the ovarian differentiation and induce masculinization through different regulatory mechanisms, which provides a fundamental insight into the sex control breeding in aquaculture.

Keywords: *Trachinotus ovatus*; transcriptome; letrozole; 17α-methyltestosterone

Key Contribution: Different molecular regulatory mechanisms to inhibit ovarian differentiation and induce masculinization after letrozole and 17α-methyltestosterone treatment in golden pompano.

check for updates

Academic Editors: Roberto Ferreira Artoni and Eric Hallerman

Received: 4 December 2024
Revised: 31 December 2024
Accepted: 3 January 2025
Published: 6 January 2025

Citation: Zhou, Q.; Wang, Y.; Guo, Y.; Li, G.; Wang, T.; Chen, H. A Comparative Transcriptome Analysis Reveals the Effects of Letrozole and 17α-Methyltestosterone on the Expression of Reproductive-Related Genes in Golden Pompano (*Trachinotus ovatus*). *Fishes* **2025**, *10*, 21. https://doi.org/10.3390/fishes10010021

Copyright: © 2025 by the authors. Licensee MDPI, Basel, Switzerland. This article is an open access article distributed under the terms and conditions of the Creative Commons Attribution (CC BY) license (https://creativecommons.org/licenses/by/4.0/).

1. Introduction

Sex plays a crucial role in both theoretical and practical scientific research, particularly in the study of sex determination mechanisms and the application of sexual dimorphism [1,2]. The genetic anatomy of the sexual regulatory mechanism will provide a theoretical foundation for reproduction strategies and sex control approaches [3,4]. Compared to mammals and birds, teleosts exhibit diverse and variable sex-determining mechanisms, including genotypic sex determination, environmental sex determination, and genotypic sex determination influenced by environmental factors [4]. Over the past few decades, exogenous hormones and other environmental conditions have been used to induce sex reversal for sex control breeding in various fish species with significant sexual dimorphism [5], such as yellow catfish (*Pelteobagrus fulvidraco*) [6] and Nile tilapia (*Oreochromis niloticus*) [7]. Aromatase inhibitor letrozole (LZ) and 17α-methyltestosterone (MT) were widely applied for masculinization in aquaculture [8–10]. However, studies on the molecular regulatory mechanisms of LZ and MT are still limited.

Aromatase (Cyp19), a key enzyme in sexual differentiation, can be produced in either the gonad or the brain [11,12]. LZs pharmacological mechanism involves the inhibition of aromatase activity, which hinders the conversion of androgens into estrogen [13]. Previous reports indicated that treatment of common carp (*Cyprinus carpio*) with 200 mg/kg LZ resulted in an outcome of 98.5% males [14]. Additionally, feeding coral trout (*Plectropomus leopardus*) a diet with 200 mg/kg LZ resulted in the successful induction of the pseudomales [15]. And research found that in Nile tilapia, LZ dose-dependently increased the percentage of males when used from 0 to 200 mg/kg, and when it exceeded 200 mg/kg the percentage of males remained fairly constant (92.5–96.0%) [16]. LZ is currently an effective drug used in studies designed to reverse sex.

MT is a synthetic androgen that can act directly on the gonad with the androgen receptor [17]. Research shows that MT exposure masculinizes female fish by affecting sex steroid hormone levels, including 11-ketotestosterone (11-KT) [18]. Similarly, yellow drum (*Nibea albiflora*) exhibited complete sex reversal at a concentration of 0.2 µg/L of MT, without any abnormalities in gonadal development [19]. In yellowtail tetra (*Astyanax lacustris*), masculinization occurred after MT treatment [20]. A related study has shown that steroidogenic acute regulatory protein (*star*), 11β-hydroxysteroid dehydrogenase 2 (*11β-hsd2*), and cytochrome P450 aromatase (*cyp19a1a*) are considered as the key genes mediating the effects of MT [21].

Research has shown that the reproductive processes in animals are primarily regulated by the hypothalamic–pituitary–gonadal (HPG) axis, a critical component of the endocrine system. Female follicular development, egg maturation, ovulation, and male spermatogenesis are largely controlled by the HPG axis [22]. In addition to the hypothalamus and the gonads, the liver influences the reproductive axis by regulating the metabolism of sex steroids [23]. However, the roles of LZ and MT in the reproduction of the golden pompano (*Trachinotus ovatus*) remain largely unexplored.

The golden pompano is widely distributed across various oceans, including the East China Sea, South China Sea, and Yellow Sea. Renowned for its tender and flavorful meat, this species is highly favored by both aquaculturists and consumers. Due to its rapid growth and ease of cultivation, the commercial breeding of golden pompano has expanded, establishing it as a key marine aquaculture species in China. According to data from the 2024 edition of the China Fishery Statistical Yearbook (National Bureau of Statistics of China, https://www.stats.gov.cn/, accessed on 4 December 2024), the golden pompano has the largest production (292,000 tons in 2023) of any commercial marine fish species in China. Observations reveal that golden pompano exhibits significant sexual dimorphism, with female individuals showing faster growth rates than their males. Increasing the proportion

of female golden pompano during the breeding process would greatly benefit the industry. Research on the transcriptome of undifferentiated gonads is crucial for identifying early sex differentiation genes. Furthermore, the assembly of the whole genome sequence of the golden pompano serves as a reference for transcriptome sequencing in this study [24].

To investigate the effects of LZ and MT on sex differentiation in golden pompano, in this study we performed comparative transcriptome analysis of the hypothalamus, the gonad, and the liver of larval fish after LZ and MT treatment. This research aims to provide a theoretical foundation for future research on the regulation of sex in golden pompano.

2. Materials and Methods

2.1. Animals

2.1.1. Fishes

The golden pompano used in the experiment was temporarily housed and treated with pharmaceuticals at the Huangliu Base of Hainan Blue Liang Technology Co., Ltd (Ledong, China). In late March 2023, spawning was induced by stimulating the mature gonads of the fish. Eggs from female fish and sperm from male fish were collected for artificial fertilization. The fertilized eggs were incubated in outdoor ponds with a salinity of approximately 31‰. At 30 days post-hatching (dph), the experimental fish (average body length of 12.73 ± 1.57 mm) were transferred to a pool measuring 4.7 m × 4.7 m × 1.7 m and randomly assigned to one of three groups. Each group was initially made up of potential males and females and contained 3000 fish. Both LZ and MT were purchased from Sigma-Aldrich (St. Louis, MO, USA). The three groups were the LZ treatment group (Group A) (n = 3), the MT treatment group (Group B) (n = 3), and the control group (Group C) (n = 3). LZ and MT were dissolved in anhydrous ethanol to form an initial solution. A precise amount of the initial solution was mixed with ethanol again and sprayed onto the feed (Fuzhou Haima Feed Co., Ltd., Fuzhou, China), which was then thoroughly stirred. The feed was subsequently freeze-dried to prepare the induction feed. Group A received feed sprayed with LZ, Group B with MT, and Group C with ethanol alone (no drugs). Both LZ and MT were administered at a concentration of 200 μg/g of feed (Figure 1). The juvenile fish were reared under natural photoperiod conditions between 28.8 and 32.2 °C. During this period, the fish were fed to satiation twice daily, at 8:00 and 16:00. After each feeding, any remaining bait and debris were removed.

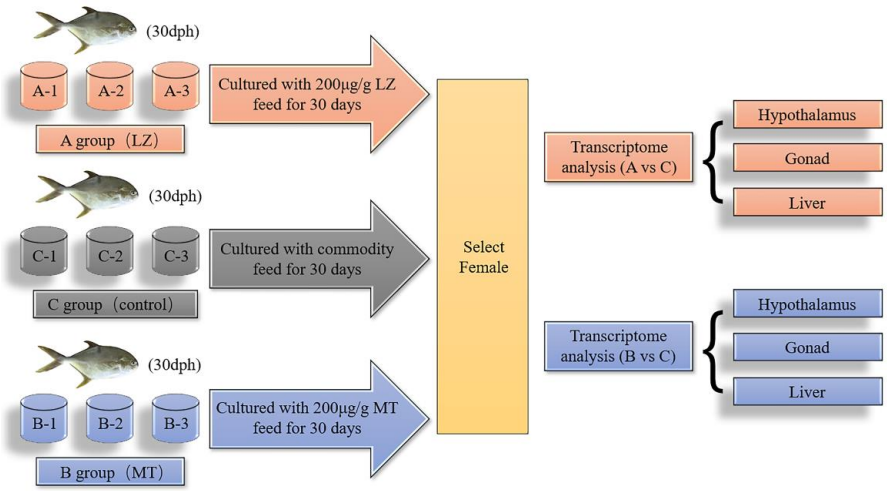


Figure 1. The detailed procedure for the treatment of golden pompano by LZ or MT.

2.1.2. Collection of Samples

At 60 dph, females and males cannot be distinguished by appearance. In order to ensure an adequate number of females for sampling, 15 fish individuals from each group were randomly selected and anesthetized using a 1% eugenol solution (E809010, Macklin Biochemical, Shanghai, China). The abdomen of each juvenile fish was dissected, and the hypothalamus, the gonad, and liver tissues were removed and placed in 2.0 mL Eppendorf tubes containing sample stabilizer (Accurate Biology Engineering Co., Ltd., Changsha, China). The samples were then stored at −80 °C until RNA extraction. To determine the genetic sex of each fish, a small sample of caudal fin tissue was collected and stored in a 2.0 mL tube filled with 100% ethanol, which was kept at −20 °C.

2.2. Identification of Genetic Sex

Before RNA extraction for RNA-seq and quantitative real-time PCR (qRT-PCR), genetic sex determination was performed. DNA was extracted from caudal fin tissue using a marine animal genomic DNA extraction kit (Guangzhou Aipuer Biotechnology Co., Ltd., Guangzhou, China), following the manufacturer's instructions. Polymerase chain reaction (PCR) amplification targeted sex-specific single nucleotide polymorphism (SNP) markers, using primers detailed in Table S1 [25]. The PCR products were sequenced using the Sanger method, and the genetic sex was determined from the sequencing map [25].

2.3. Transcriptome Analysis

2.3.1. RNA Extraction and Sequencing

The hypothalamus, the gonad, and liver tissues from female juvenile fish were used as experimental materials, with three biological replicates per group (n = 27). A TRIzol reagent kit was used to determine RNA degradation and contamination by 1.5% agarose gel electrophoresis. RNA purities and concentration were assessed with an Agilent 2100 Bioanalyzer (Agilent Technologies Inc., Santa Clara, CA, USA) and a NanoDrop 2000c spectrophotometer (Thermo Fisher Scientific, Waltham, MA, USA). The extracted RNA was then used for RNA-seq. The sequencing library comprises LZ-treated Hy-A, Go-A, and L-A; MT-treated Hy-B, Go-B, and L-B; and a control group consisting of Hy-C, Go-C, and L-C. Eukaryotic RNA was enriched using magnetic beads with Oligo (dT), followed by the addition of a fragmentation buffer to randomly fragment the RNA. Subsequently, the first cDNA strand and the second strand were synthesized using RNA as a template, and the cDNA was purified. The purified double-stranded cDNA was then subjected to end-repair, A-tailing, and connection to sequencing adapters. Fragment size selection is carried out using AMPure XP beads. Finally, the cDNA library was obtained through PCR enrichment.

Upon the completion of library construction, the Qubit 3.0 Fluorometer (Thermo Fisher Scientific, Waltham, MA, USA) was used for preliminary quantification, with the concentration required to exceed 1 ng/μL. The Qsep400 High-Throughput Analysis System (Bioptic Inc., Taiwanese, China) was then employed to assess the insertion fragments of the library. Once the fragment insertions met expectations, qRT-PCR was performed to accurately quantify the effective library concentration (greater than 2 nM) to ensure quality. After passing quality control, the libraries were sequenced in PE150 mode on the Illumina NovaSeq6000 platform (San Diego, CA, USA). Data analysis was conducted using the bioinformatics pipeline provided by the BMKCloud (http://www.biocloud.net/, accessed on 4 December 2024) platform. Readings containing low-quality sequences were removed, and the downstream data were filtered to yield clean data. Finally, clean data were compared with the genome of golden pompano and proceeded to the next step of analysis.

2.3.2. Functional Enrichment Analysis

The gene expression level was calculated using the FPKM (fragments per kb per million reads) method. Fold change (FC) represents the ratio of expression levels between the two groups. DEGs analysis was conducted using DEseq2 v3 software (https://github.com/genepattern/DESeq2/, accessed on 4 December 2024). A gene was considered differentially expressed when $|\log2(FC)| \geq 1$ and p value ≤ 0.05. Functional annotation of databases of genes that are differentially expressed, such as the Gene Ontology (GO) functional annotation of differential genes and the Kyoto Encyclopedia of Genes and Genomes (KEGG) pathway enrichment, were performed using Biomark online tools (http://www.biocloud.net/, accessed on 4 December 2024). The significance of enrichment analysis was indicated by $p < 0.05$.

2.4. qRT-PCR

Each data set was randomly selected to include 8 to 10 relevant genes, and the RNA-seq results were validated using qRT-PCR. Primers were designed using Primer Premier 5.0 software and synthesized by Sangon Bioengineering Co., Ltd. (Shanghai, China), as detailed in Table S1. qRT-PCR was performed on DEGs, with *β-actin* used as the internal reference gene. Total RNA was extracted from three sets of samples—the hypothalamus, the gonad, and the liver (27 samples in total) using the TRIzol reagent as discussed previously in this study. cDNA was synthesized via reverse transcription following the TransScript® Fly First-Strand cDNA Synthesis SuperMix kit (Beijing TransGen Biotech Co. Ltd., Beijing, China) protocol. The qRT-PCR reactions were conducted on a Roche Light Cycler 480 II real-time PCR system, using the PerfectStart® Green qPCR SuperMix kit (Beijing TransGen Biotech Co., Ltd., Beijing, China), according to the manufacturer's instructions. Reactions were carried out in a total volume of 10.0 μL, comprising 5.0 μL of PerfectStart® Green qPCR SuperMix, 0.4 μL of each forward and reverse primer, 3.2 μL of DNase/RNase-free H_2O, and 1.0 μL of cDNA template. Thermal cycling conditions were as follows: initial denaturation at 94 °C for 2 min, followed by 40 cycles of 94 °C for 20 s, 58 °C for 20 s, and 72 °C for 20 s. The relative expression of DEGs was calculated using the $2^{\Delta\Delta Ct}$ method.

3. Results

3.1. Sequencing Results of Transcriptome Reads

To investigate the alterations in reproductive-related genes influenced by LZ or MT, we sequenced 27 cDNA libraries derived from the hypothalamus, the gonads, and the liver of golden pompano. The sequencing results for the hypothalamus transcriptome revealed a total of 56,464,047,246 high-quality bases. The Hy-A, Hy-B, and Hy-C groups yielded 62,408,125, 62,089,326, and 64,504,851 high-quality sequence fragments, respectively. The sequencing quality value for Q20 exceeded 97.95% in all groups, while Q30 exceeded 94.61%. The GC content ranged from 45.22 to 45.47%. For the gonad transcriptome, the sequencing revealed a total of 56,479,636,684 high-quality bases. The Go-A, Go-B, and Go-C groups produced 62,226,912, 62,304,807, and 64,372,839 high-quality sequence fragments, respectively. Q20 exceeded 98.01% for all groups, while Q30 was above 94.76%. The GC content ranged from 47.49 to 50.37%. For the liver transcriptome, 59,864,108,374 high-quality bases were obtained. The L-A, L-B, and L-C groups produced 73,205,006, 62,263,256, and 64,495,109 high-quality sequence fragments, respectively. Q20 exceeded 98.03%, while Q30 surpassed 94.05%. The GC content ranged between 48.96 and 49.88%. The data meet requirements, and the quality of the sequencing is generally high enough for subsequent analysis (Table S2).

3.2. Differential Expression Analysis

Gene expression levels were normalized using FPKM values. DEGs in the hypothalamus, the gonad, and the liver tissue of control female golden pompano and those exposed to LZ and MT were identified based on $|\log_2(FC)| \geq 1$ and $p \leq 0.05$. The distribution of these expression levels is depicted in a series of box plots (Figures 2, 3 and 4A). The overlap of DEGs between the two groups is visualized using Venn diagrams (Figures 2, 3 and 4B), which highlights a limited number of common DEGs across the respective comparison groups under the two conditions. The expression profiles of all DEGs were further analyzed through a heatmap (Figures 2, 3 and 4C,D), which revealed different expression patterns under the influence of LZ and MT.

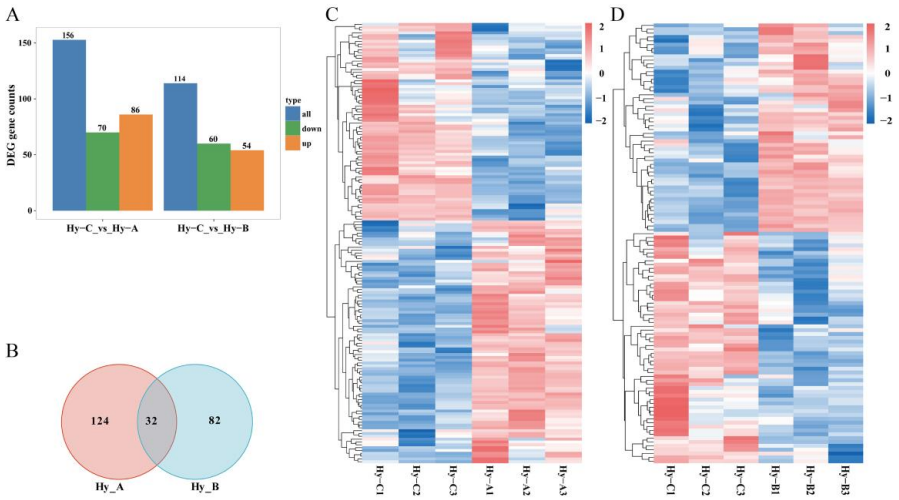


Figure 2. Analysis of gene expression patterns in hypothalamus tissues of the golden pompano. (**A**) Number of DEGs. (**B**) Venn diagrams showing the distribution of DEGs under the influence of LZ and MT. (**C**,**D**) Heatmap indicates the expression levels of all DEGs in the Hy-A and the Hy-B groups throughout processing periods.

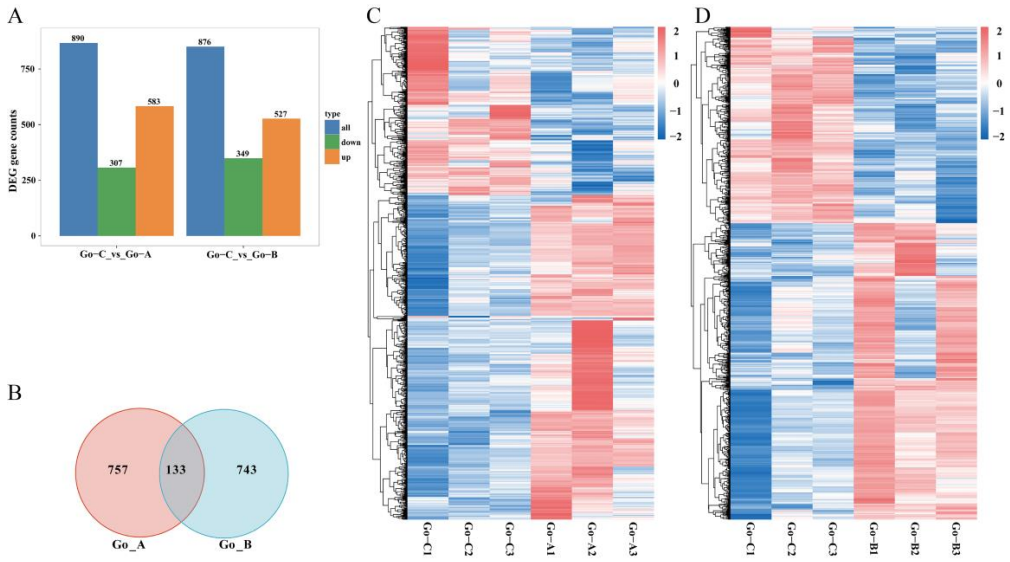


Figure 3. Analysis of gene expression patterns in gonad tissues of the golden pompano. (**A**) Number of DEGs. (**B**) Venn diagrams showing the distribution of DEGs under the influence of LZ and MT. (**C**,**D**) Heatmap indicates the expression levels of all DEGs in the Hy-A and the Hy-B groups throughout processing periods.

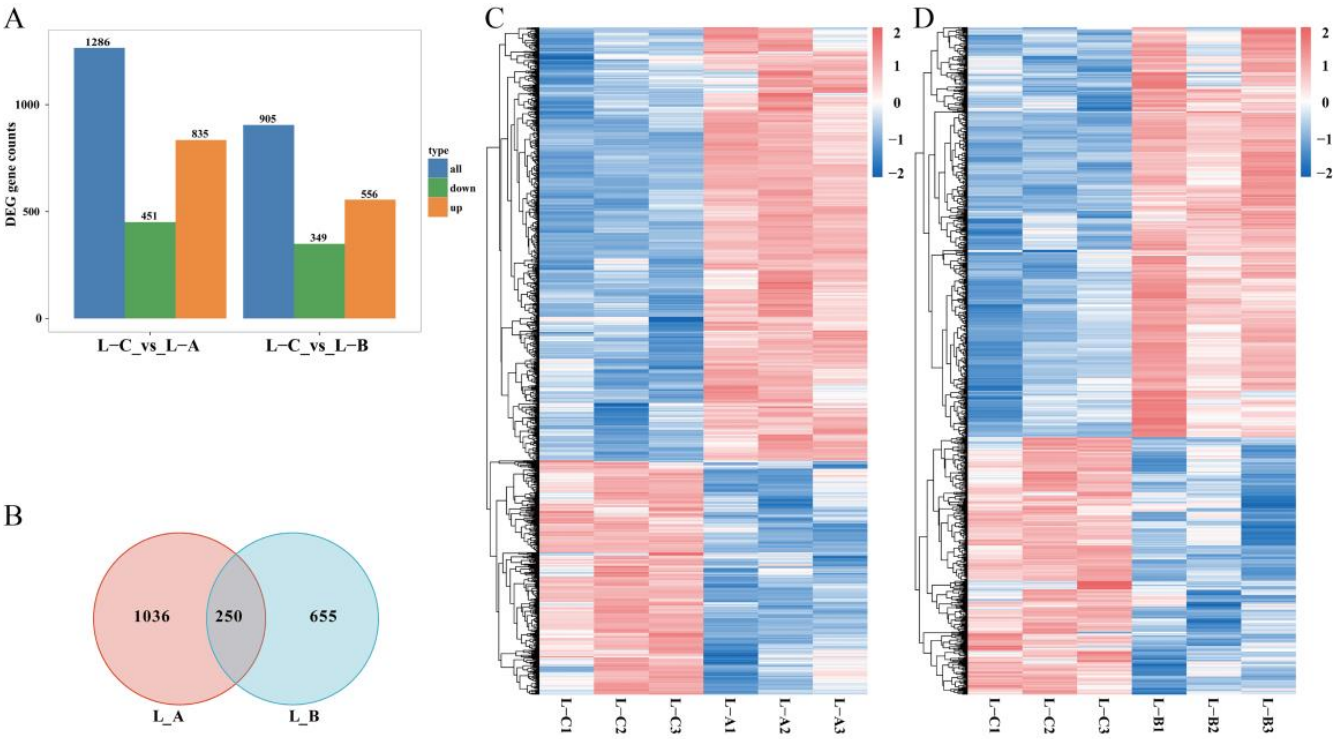


Figure 4. Analysis of gene expression patterns in liver tissues of the golden pompano. (**A**) Number of DEGs. (**B**) Venn diagrams showing the distribution of DEGs under the influence of LZ and MT. (**C**,**D**) Heatmap indicates the expression levels of all DEGs in the Hy-A and the Hy-B groups throughout processing periods.

A total of 156 DEGs were identified in the comparison between Hy-C and Hy-A, with 86 up-regulated and 70 down-regulated. In comparing Hy-C vs. Hy-B, 114 DEGs were identified, including 54 up-regulated and 60 down-regulated genes (Figure 2A). Additionally, 32 co-expressed DEGs were shared between the Hy-C vs. Hy-A and the Hy-C vs. Hy-B comparisons. Group A exhibited 124 genes with unique differences, while Group B displayed 82 genes with distinct differences (Figure 2B). The distribution of these DEGs is shown in the volcano plots (Figure 5A,B). In the comparison between Go-C and Go-A, 890 DEGs were identified, with 583 up-regulated and 307 down-regulated. In the comparison of Go-C vs. Go-B, 876 DEGs were identified, including 527 up-regulated and 349 down-regulated genes (Figure 3A). Notably, 133 co-expressed DEGs were shared between the Go-C vs. Go-A and the Go-C vs. Go-B comparisons. Group A exhibited 757 unique genes, while Group B showed 743 specific genes (Figure 3B). The distribution of these DEGs is illustrated in volcano plots (Figure 5C,D). A total of 1286 DEGs were identified in the comparison between L-C and L-A, with 835 up-regulated and 451 down-regulated. In comparing L-C vs. L-B, 905 DEGs were identified, including 556 up-regulated and 349 down-regulated genes (Figure 4A). Additionally, 250 co-expressed DEGs were shared between both comparisons. Group A exhibited 1036 unique genes, while Group B displayed 655 distinct genes (Figure 4B). The distribution of these DEGs is shown in the corresponding volcano plots (Figure 5E,F).

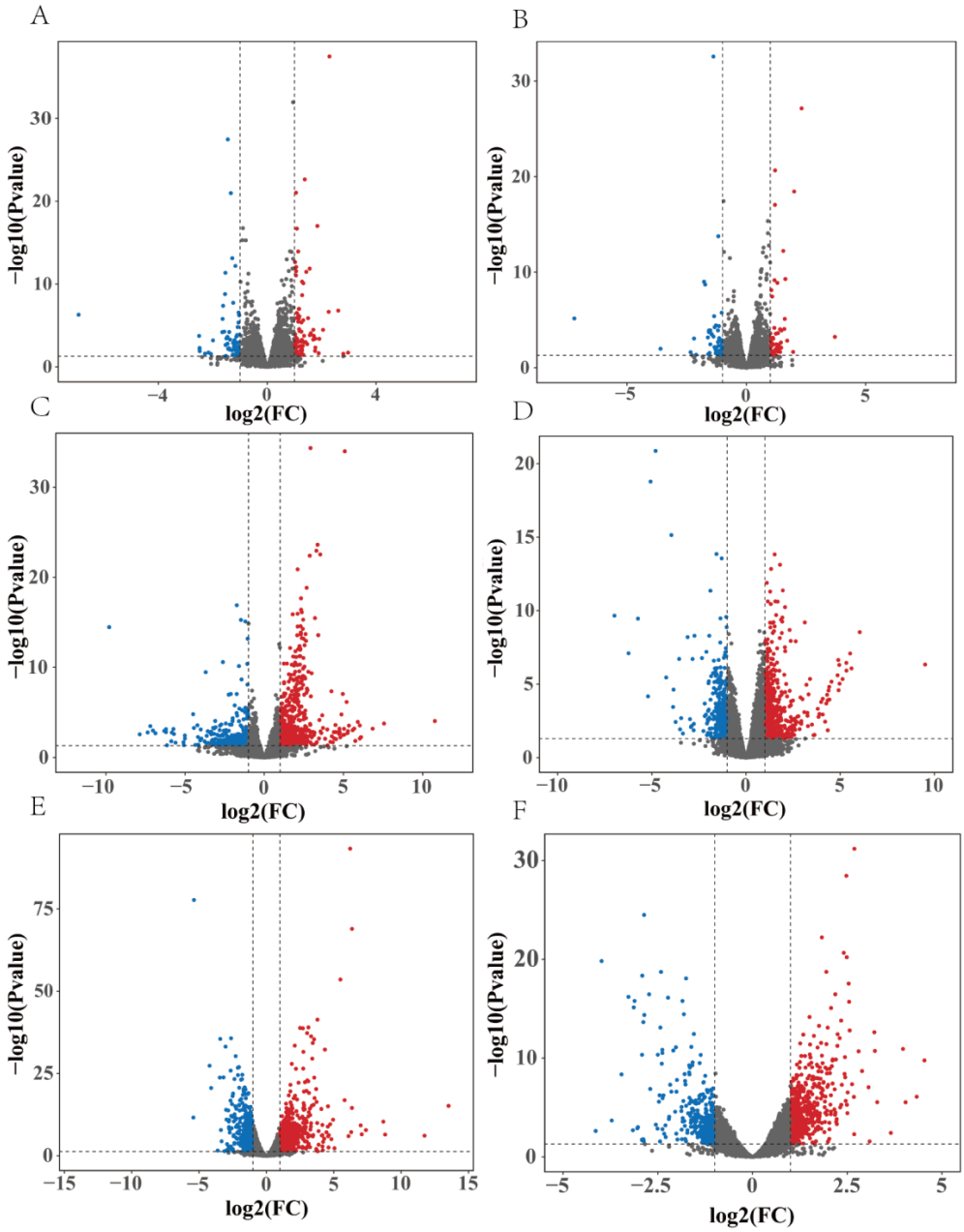


Figure 5. Volcano plots of gene expression differences. Red dots: up-regulation; blue dots: down-regulation; grey dots: normal-regulation. (**A**) Hypothalamus tissue transcriptome (LZ); (**B**) hypothalamus tissue transcriptome (MT); (**C**) ovarian tissue transcriptome (LZ); (**D**) ovarian tissue transcriptome (MT); (**E**) liver tissue transcriptome (LZ); (**F**) liver tissue transcriptome (MT).

3.3. The Enriched GO Terms Pathways

Gene Ontology (GO) enrichment analysis revealed that the differentially expressed genes were significantly enriched in three functional categories: biological process (BP), cellular component (CC), and molecular function (MF) (Figure 6). Within the BP category, the differentially expressed genes were predominantly enriched in cellular processes, biological regulation, and responses to stimuli. In the CC category, the enrichment was primarily observed in cellular anatomical entities, intracellular components, and protein-containing complexes. Finally, in the MF category, the differentially expressed genes were mainly enriched in binding and catalytic activities.

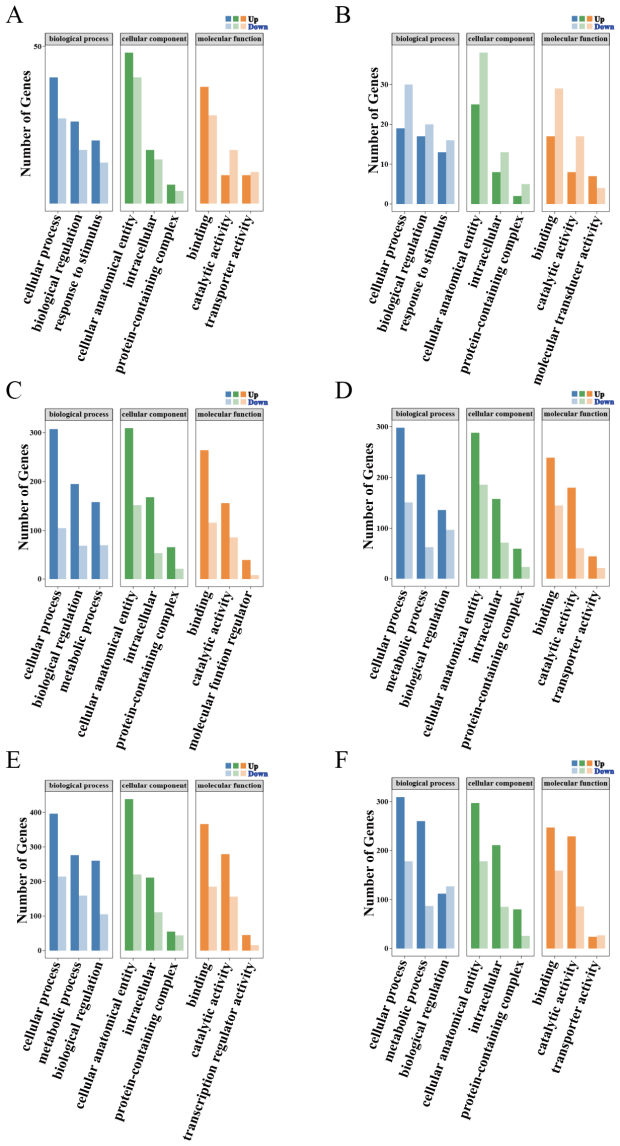


Figure 6. Functional annotation of DEGs based on GO classification. The horizontal axis indicates GO function and the vertical axis indicates the number of genes with GO function. (**A**) Pathway enrichment analysis of DEGs in the hypothalamus under the influence of LZ; (**B**) pathway enrichment analysis of DEGs in the hypothalamus under the influence of MT; (**C**) pathway enrichment analysis of DEGs in the gonad under the influence of LZ; (**D**) pathway enrichment analysis of DEGs in the gonad under the influence of MT; (**E**) pathway enrichment analysis of DEGs in the liver under the influence of LZ; (**F**) pathway enrichment analysis of DEGs in the liver under the influence of MT.

3.4. The Enriched KEGG Terms Pathways

The KEGG analysis reveals the top 20 most enriched KEGG signaling pathways in the experimental group compared to the control group (Figure 7). In the Hy-C vs. Hy-A group, the pathways with the most significant enrichment include arachidonic acid metabolism, the p53 signaling pathway, and the HIF-1 signaling pathway. The reproduction-related pathways identified are oocyte meiosis and the cell cycle. In the Hy-C vs. Hy-B group, the most significantly enriched KEGG pathways are protein digestion and absorption, retinol metabolism, and the p53 signaling pathway. The reproduction-related pathways in this group include steroid hormone biosynthesis, and the metabolism of xenobiotics by cytochrome P450. In comparing the Go-C vs. Go-A groups, the most significantly enriched KEGG pathways include the cell cycle, fructose and mannose metabolism, and renal cell

carcinoma. The reproductive-related pathways identified are oocyte meiosis, steroid biosynthesis, and progesterone-mediated oocyte maturation. In the Go-C vs. Go-B group, the most significantly enriched KEGG pathways comprise ferroptosis, biosynthesis of amino acids, and ribosome biogenesis in eukaryotes. Pathways associated with reproduction in this group include ovarian steroidogenesis, cortisol synthesis and secretion, cysteine and methionine metabolism, and steroid hormone biosynthesis. In the comparison between the L-C and L-A groups, the most significantly enriched KEGG pathways were identified as the PPAR signaling pathway, cytochrome P450, drug metabolism through other enzymes, and the metabolism of xenobiotics by cytochrome P450. In the L-C vs. L-B group, the most significantly enriched KEGG pathways were steroid biosynthesis, fatty acid metabolism, and the PPAR signaling pathway, with the reproductive-related pathways comprising steroid biosynthesis, steroid hormone biosynthesis, and drug metabolism through other enzymes.

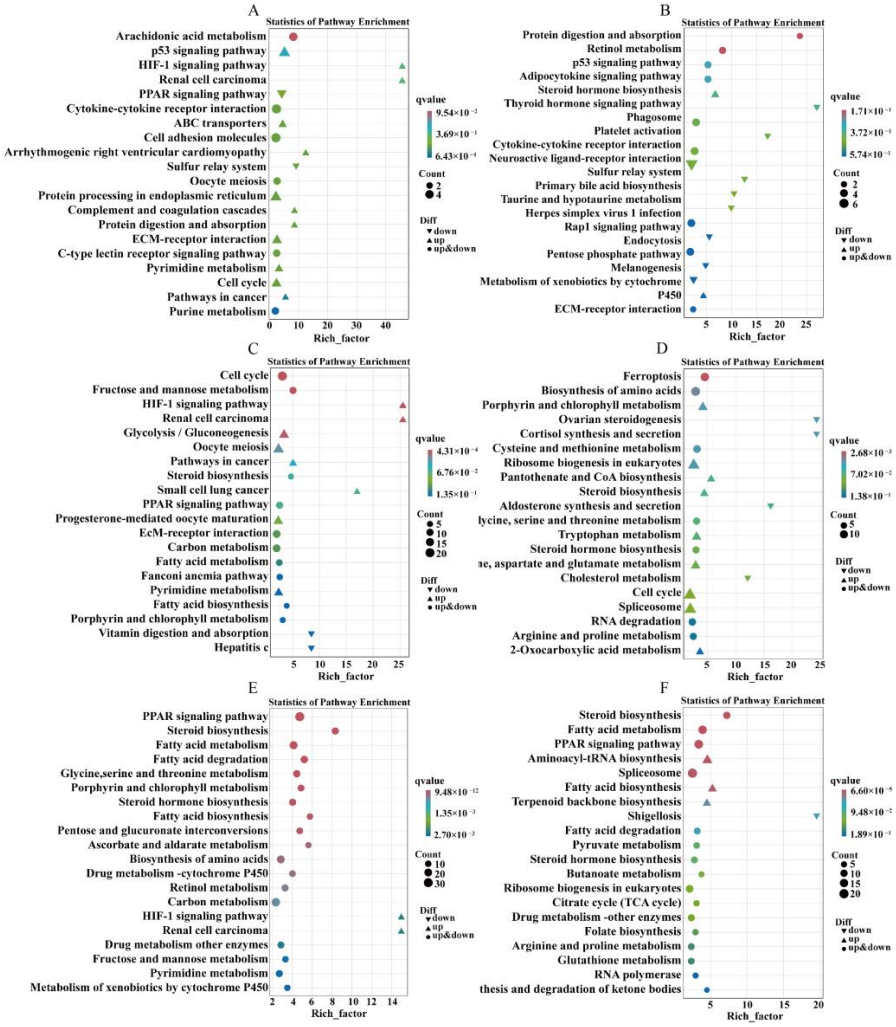


Figure 7. DEGs are significantly enriched in KEGG pathways. (**A**) LZ affects the pathway enrichment analysis of DEGs in the hypothalamus. (**B**) Pathway enrichment analysis of DEGs in the MT-influenced hypothalamus. (**C**) Pathway enrichment analysis of DEGs in the LZ-influenced hypothalamus. (**D**) Pathway enrichment analysis of DEGs in the gonad under the influence of MT. (**E**) Pathway enrichment analysis of DEGs in the liver under the influence of LZ. (**F**) Pathway enrichment analysis of DEGs in the liver under the influence of MT. Pathways and enrichment factors are indicated on the vertical and horizontal axes, respectively. The size of the dots indicates the number of genes and the color indicates the q-value.

3.5. qRT-PCR Confirmation of DEGs

To validate the findings of the RNA-seq analysis, genes associated with reproduction were randomly selected for further investigation using qRT-PCR. In the comparison of Hy-C vs. Hy-A, genes such as *spata5l1x3*, *ckap4*, *dan4lx2*, and *ccnb1* were up-regulated, while *cbln1l*, *lcnl*, *per1l*, and *adcy1l* were down-regulated. In the comparison of Hy-C vs. Hy-B, the expression levels of *loxhd1*, *lcnl*, and *cycsl* were up-regulated, while *cbln1l*, *crhr1*, *scgnlx2*, *caln1l*, and *adcy1l* were down-regulated. In the comparison of Go-C vs. Go-A, randomly selected genes such as *rsbn1l*, *cdca3*, *fstl*, *cdc20*, and *pmf1l* were up-regulated, while *chac1l*, *gadd45bl*, *cbsl*, *ctsbl*, and *enpep* were down-regulated. In the comparison of Go-C vs. Go-B, genes including *smox*, *arg1*, *sam*, *srm*, *gss*, and *enoph1* were up-regulated, while *fbxo25x1*, *bmallx1*, and *cbslx2* were down-regulated. In the comparison of L-C vs. L-A, genes such as *fmo5l*, *glul*, *elovl6l*, *fads2*, and *hsd17b7l* were up-regulated, while *cyp4503a40*, *hadhb*, *tymp*, and *got1* were down-regulated. In the comparison of L-C vs. L-B, *fasn*, *fads2a*, *fads2*, *elovl6l*, and *sams* were up-regulated, whereas *hgf*, *gys2*, *spock2x1*, *ldlr*, and *fmo5l* were down-regulated. The expression trends of all randomly selected differential genes were consistent with the RNA-seq findings (Figure 8), and the results of qRT-PCR confirmed the RNA-seq analysis.

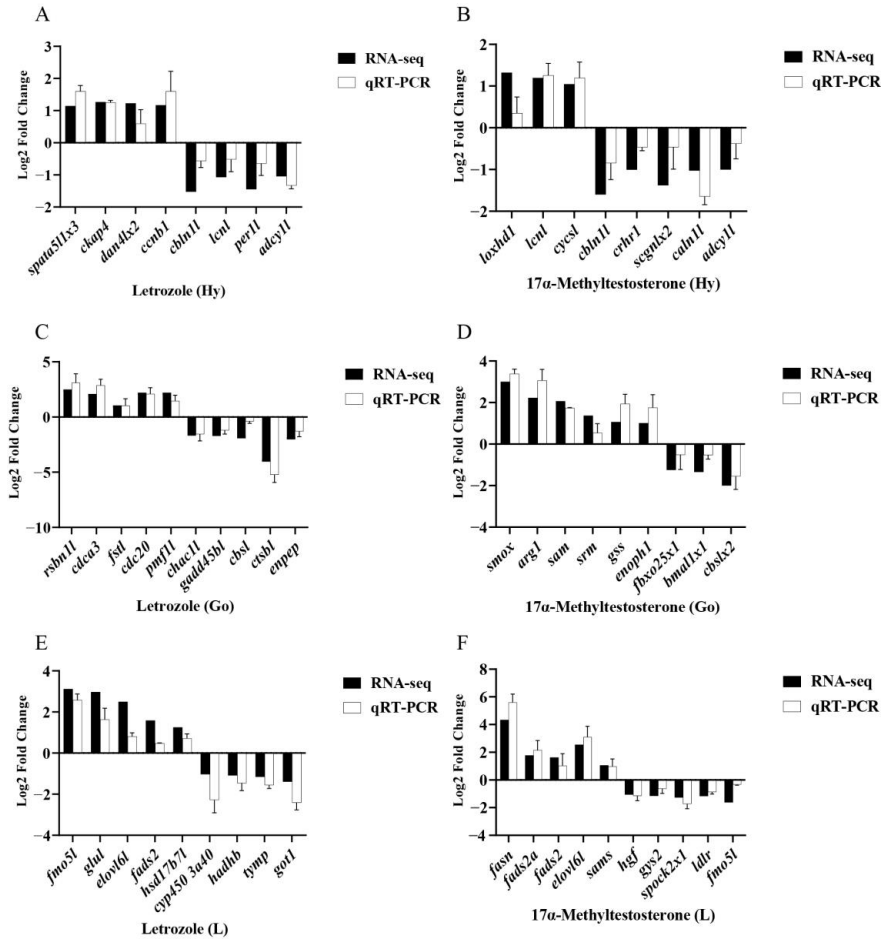


Figure 8. (**A**) The expression profiles of 8 hypothalamus genes using qRT-PCR (LZ); (**B**) the expression profiles of 8 hypothalamus genes using qRT-PCR (MT); (**C**) the expression profiles of 10 ovarian genes using qRT-PCR (LZ); (**D**) the expression profiles of 9 ovarian genes using qRT-PCR (MT); (**E**) validation of the expression profiles of 9 liver genes using qRT-PCR (LZ); (**F**) validation of the expression profiles of 10 liver genes using qRT-PCR (MT).

3.6. Effects of LZ and MT on Reproduction

To further examine the molecular mechanisms of LZ and MT on the hypothalamus, the gonad, and the liver, we analyzed the expression patterns of key DEGs in major reproductive pathways. Specifically, we assessed the expression dynamics of DEGs involved in estrogen synthesis and metabolism, oocyte meiosis, and cysteine and methionine metabolism in both treatment groups (Figures 9 and 10). The results indicated a significant upregulation of genes related to oocyte meiosis in the gonads under the influence of LZ, including *plk1*, *fbxo43*, *fbxo5*, *bub1*, *sgo*, and *securin*. Additionally, genes associated with cysteine and methionine metabolism, such as *sam*, *srm*, *looa*, and *enoph1*, were notably up-regulated in response to MT exposure. Significant changes were also seen in genes involved in estrogen synthesis and metabolism, such as *sqle*, *cyp3a40*, *ugt1a1*, *ugt2a1*, *ccnb1*, *securin*, *cdkn1a*, *hsd17b7*, *cyp1a*, and *cyp19a1*.

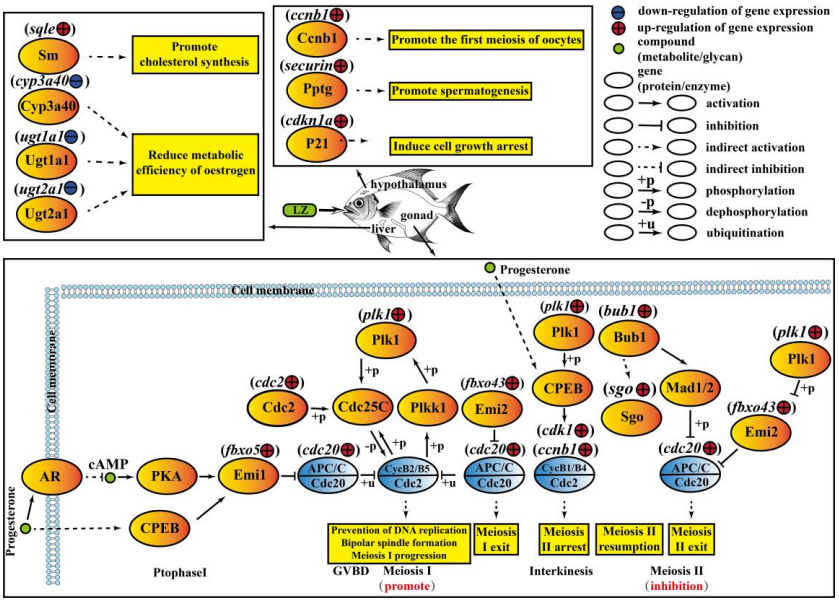


Figure 9. Reproduction-related DEGs under the influence of LZ.

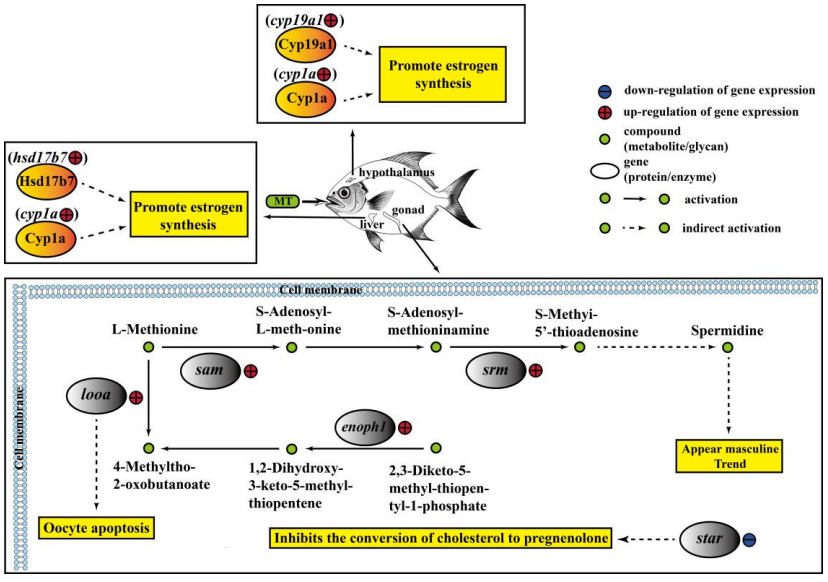


Figure 10. Reproduction-related DEGs under the influence of MT.

4. Discussion

In the development of fish gonads, sex hormones are extremely important. Aromatase catalyzes the final step in estrogen synthesis, converting androstenedione and testosterone into estrone and estradiol, respectively. Its activity regulates the balance of androgens and estrogens during gonadal development. Study has shown that oocyte growth, maturation, and ovulation are critical for successful reproduction, with oogenesis being predominantly regulated by estrogen and progesterone at the gonadal level [26]. However, there is limited research on the effects of LZ and MT on the reproduction of golden pompano. Therefore, this study utilized RNA-seq technology to explore the molecular mechanisms of LZ and MT on the hypothalamus, the gonad, and liver tissues of golden pompano.

4.1. LZ Can Affect Oocyte Meiosis and Estrogen Metabolism

In hypothalamus tissue affected by LZ, the expression of genes related to sex differentiation in the Hy-A group, including *ccnb1*, *securin*, and *cdkn1a*, was altered. Activated Ccnb1 promotes the transition from the G2 to M phase, initiating mitosis [27]. Research showed that Ccnb1 plays a key role in oocyte meiosis [28]. Additionally, disruption of Ccnb1 in oocytes has been linked to germ cell depletion and infertility [29]. In this study, the expression of this gene was up-regulated, suggesting that LZ may promote the first meiosis of oocytes. Securin is encoded by the pituitary tumor-transforming gene (*pttg*). Studies have shown that *pttg* is exclusively expressed in the testis, particularly in spermatocytes and sperm cells during specific developmental stages, playing an essential role in spermatogenesis [30,31]. Consequently, the up-regulation of *pttg* indicates that the development of the ovary is influenced by the action of the LZ, with the appearance of testis characteristics. In addition, P21 (Cdkn1a) is critical in regulating cell cycle progression. At low concentrations, P21 enhances the formation and kinase activity of the Cdk4/Cyclin D1 complex, though some studies suggested that P21 can also induce cell growth arrest [32,33]. In this study, the up-regulation of *cdkn1a* was observed, but its specific function warrants further investigation.

The transcriptome of ovarian tissue was subsequently analyzed. The results indicated that the expression levels of several genes associated with oocyte meiosis changed, including *fbxo5*, *fbxo43*, *plk1*, *cdc20*, *cdk1*, *ccnb1*, *sgo1*, and *bub1*. The expression levels of *fbxo5* and *fbxo43* were significantly up-regulated under the influence of LZ. Fbxo5, also known as early mitosis inhibitor-1 (Emi1), encodes a member of the F-box protein family and serves as a critical regulatory gene in the cell cycle. It plays a significant role in regulating S phase progression and mitosis by inhibiting the anaphase-promoting complex (APC) mechanism [34,35]. The activity of the anaphase-promoting complex/cyclosome (APC/C) is a crucial factor in germinal vesicle breakdown (GVBD) and metaphase II (MII) of meiosis during the maturation of vertebrate oocytes [36]. The expression of Emi1 correlates with the proliferative status of cellular compartments, and cells deficient in Emi1 undergo cellular senescence [37]. In mouse oocytes, the microinjection of excess Emi1 leads to a significant arrest at the metaphase of the first meiotic division (MI) [38]. Consequently, elevated levels of Emi1 may facilitate the first meiotic division of golden pompano oocytes while inhibiting the transition from MI to MII. Fbxo43 is an important paralog of Fbxo5, also known as early mitosis inhibitor-2 (Emi2). It controls cell-cycle-protein stability and the stagnation of the MII stage [38]. In this study, we observed a significant up-regulation in the expression of the *fbxo43*. This finding further illustrates that the elevated expression of *fbxo5* and *fbxo43* facilitates the development of oocytes into MI while preventing their progression into MII. In this pathway, the expression of the *plk1* and *cdc20* was also up-regulated in response to LZ stimulation. The regulation of cell meiosis is mediated by polo-like kinase (Plk). Plk1, a member of the serine/threonine protein kinase family, plays a crucial role in various

stages of mitotic progression, including the regulation of centrosome maturation, mitotic spindle formation, and cytokinesis [39]. Studies have demonstrated that the expression of Plk1 is dependent on the cell cycle. It typically accumulates at the centrosome of the spindle during the early stages of mitosis and subsequently migrates gradually from the spindle to the equatorial plate. Plk1 expression is notably low during the G0, G1, and S phases, and remains low in the G2 phase. However, it begins to increase and reaches its peak during the M phase [40]. Plk1 facilitates this process by phosphorylating Cdc20, thereby maintaining its association with the mitotic checkpoint complex (MCC) until all kinetochores are properly attached to the mitotic spindle fibers. Cdc20 plays a crucial role in cell cycle progression and chromosome segregation through its APC/C-mediated function [41]. Furthermore, evidence suggested that the overexpression of Cdc20 in normal cells promotes cell growth and inhibits apoptosis [42], which aligned with the expression effects observed for Emi1 and Emi2. Plk1 and Cdc20 may be involved in cell division during the MI stage of oocyte development, playing a crucial role in this process. However, it has also been shown that Plk1 and Cdc20 are also significant genes in regulating male post-meiotic spermatogenic cell development and sperm quality [43]. LZ's inhibitory effect on aromatase activity hinders the conversion of androgens into estrogens, promoting an increase in endogenous gonadotropin secretion, which may facilitate the first meiotic division of oocytes. Nevertheless, the inhibition of estrogen conversion may lead to a relative increase in androgen levels within the ovary, potentially stimulating the transformation of ovarian tissue into testicular tissue. This finding aligns with the results obtained from the aforementioned hypothalamus transcriptome analysis.

The study showed that the expression of two key factors, cyclin-dependent kinase 1 (Cdk1) and cyclin B, was increased when *plk1* was expressed [44]. Cdk1, also known as cell division control protein 2 (Cdc2), is essential for the transition from the G2 phase to mitosis. It remains inactive until late G2, when cyclin B is expressed at high levels, allowing for the stable formation of the Cdk1–cyclin B complex [45]. During mid-division, Cdk1 primarily creates phosphorylation docking sites for Plk1, while the cyclinB1/Cdk1 complex plays a specific regulatory role that prompts cells to enter mitosis. Additionally, Cdk1 is involved in mitochondrial fission and the G2/M transition, coordinating mitochondrial bioenergy to ensure a smooth transition and successful cell division [46]. Ccnb1 is a crucial member of the cyclin family. Activated Ccnb1 facilitates the transition of cells from the G2 phase to the M phase, thereby initiating the process of mitosis [27]. However, studies indicated that cyclin B is degraded during the transition from MI to MII. In the oocyte meiosis pathway, the expression levels of *cdk1* and *ccnb1* were also up-regulated, mirroring the expression patterns of *plk1* and *cdc20* mentioned previously. This up-regulation is closely associated with the function of *plk1*, which maintains the cohesion of *sgo1* and *bub1* at the centromere during the prophase, metaphase, and anaphase stages, both of which are critical for chromosome segregation [47,48]. Comparative studies used Reads Per Kilobase per Million mapped readings (RPKM) which have revealed that genes such as *cdk1*, *ccnb1*, *cdc20*, *bub1*, and *sgo1* are expressed in the gonads; however, their expression levels in testes were significantly higher than those in ovaries [49]. This again suggests that the ovarian tissue of golden pompano may have undergone masculinization due to the influence of LZ.

In addition to their action on the hypothalamus and the gonads, sex hormones also significantly target another organ: the liver. Research has shown that the hormones are distributed equally in reproductive and non-reproductive tissues [50]. In the liver tissue transcriptome influenced by LZ, multiple KEGG pathways associated with reproduction were significantly enriched, including steroid biosynthesis, steroid biohormone synthesis, drug metabolism-cyp450, cyp450 metabolism of exogenous compounds, and drug metabolism involving other enzymes. Within these pathways, genes such as *sqle*, *cyp3a40*,

ugt1a1, *ugt2a1*, and *ugt2c1* were associated with the synthesis of sex hormones, and their expression levels exhibited significant alterations. Squalene monooxygenase (Sm), encoded by the *sqle*, catalyzes the conversion of squalene into 2,3 (S)-monoxysqualene. This enzyme was recognized as one of the rate-limiting factors in the cholesterol synthesis pathway and exhibited high expression levels in the liver and testes [51]. In this study, we observed an up-regulation of this gene, suggesting that LZ may enhance the cholesterol synthesis process. *Cyp3a40*, *ugt1a1*, *ugt2a1*, and *ugt2c1* were all implicated in the synthesis of estrogen. Cyp3a40 is one of the isoenzymes within the Cyp3a family, which demonstrates high catalytic activity for the hydroxylation of sex steroids [52]. Specifically, Cyp3a4, Cyp3a5, and Cyp3a11 exhibited significant catalytic activity toward estrogen [53,54]. Additionally, certain UDP-glycosyltransferases (UGT), such as UGT1A1 [55] and UGT2A1 [56], were known to catalyze the glucuronidation of endogenous estrogens. In this study, analysis revealed that the expression levels of *cyp3a40*, *ugt1a1*, and *ugt2a1* were all down-regulated, suggesting a reduction in the metabolic efficiency of estrogen. This decrease may be attributed to the inhibition of aromatase expression by LZ, which prevents the conversion of androgens into estrogens. Consequently, the reduced estrogen synthesis may lead to a relatively diminished metabolic efficiency in female fish compared to normal female fish.

In summary, LZ primarily affects oocyte meiosis in golden pompano. Transcriptome analysis of the hypothalamus and the liver revealed significant changes in cholesterol synthesis and estrogen metabolism genes.

4.2. MT Affects Amine Synthesis and Sex Hormone Metabolism

In the Hy-B group, exposure to MT increased the expression of genes associated with sex steroid hormone synthesis, such as *cyp19a1* and *cyp1a*. It is important to note that sex steroid hormones are synthesized not only in the gonads but also in the brain. Furthermore, estrogen plays a crucial role in male development. The expression of aromatase in the male hypothalamus peaked around birth, which was critical for sexual differentiation in fish [57]. In the male gonad, estrogen is produced in Leydig cells, Sertoli cells, and mature spermatocytes [58]. Notably, the knockout of *cyp19a1* resulted in male sterility [59]. The cyp1a family primarily comprises cyp1a1 and cyp1a2, both of which are involved in estrogen regulation [53]. These findings indicated that the expression of aromatase genes is enhanced in golden pompano when fed an MT complex diet. Given that estrogen is vital for testicular development, it is insufficient to study only hypothalamus tissue to assess the impact of MT on gonadal differentiation in golden pompano; further analysis of gonadal tissue is necessary.

In the gonads tissue of golden pompano, under the influence of MT, according to the KEGG enrichment analysis, significant differences were observed in the genes associated with the metabolism of cysteine and methionine, including *enoph1*, *sams*, *srm*, *gss*, *laao*, and *gss*. Enoph1 is involved in the biological synthesis of polyamines [60]. S-adenosylmethionine synthase (Sams), encoded by the *sams*, catalyzes the synthesis of S-adenosylmethionine (Sam) from methionine and ATP [61]. Sam plays a critical role in the biological synthesis of polyamines. In this study, the expression of *enoph1* and *sams* was found to be up-regulated, suggesting that the presence of MT enhances the synthesis of polyamine substances in the gonads of golden pompano. Previous research has indicated that naturally occurring polyamines are vital growth factors in eukaryotic cells. The physiological functions of polyamines encompass nucleic acid packaging, regulation of gene expression, and the modulation of cell proliferation, differentiation, and development [62]. Thus, it is evident that the synthesis of polyamines is essential during gonadal development. In addition to *sams*, another gene involved in the synthesis of polyamines, *srm*, is also up-regulated. The spermidine synthase encoded by *srm* is one of the four enzymes in the

polyamine synthesis pathway and regulates the final step of spermidine synthesis. This enzyme catalyzes the conversion of putrescine to spermidine, utilizing decarboxylated S-adenosylmethionine as a cofactor. Spermidine was first extracted from semen and is essential for growth and development [63]. Relevant research indicated that supporting cells and interstitial cells can synthesize spermidine during spermatogenesis [64]. Therefore, MT may influence the ovarian tissue of the golden pompano, prompting the ovary to synthesize polyamines primarily composed of spermidine, thereby facilitating the transformation of the ovary into testis. The pathway was also found which confirmed that the expression of *laao* and *gss* was significantly up-regulated. *Laao* possesses potential apoptosis-inducing activity in certain fish species [65]. Gss facilitates the synthesis of glutathione (Gsh), which plays a central role in apoptosis [66]. This suggests that MT may induce oocyte apoptosis.

In the pathway of ovarian steroidogenesis, *star* showed significant changes. Steroidogenic acute regulatory protein (Star) primarily mediates the rate-limiting step in steroid biosynthesis, which involves the transport of cholesterol, the substrate for all steroid hormones from the outer mitochondrial membrane to the inner mitochondrial membrane. Once in the inner membrane, cytochrome P450 cholesterol side chain cleavage enzyme (P450scc) cleaves the cholesterol side chain to produce pregnenolone, the first steroid [67]. Pregnenolone serves as a crucial intermediate in the synthesis of progesterone, finasteride, and other steroid hormones. Additionally, related studies have demonstrated that the downregulation of the *star* is associated with the inhibition of progesterone production in cells induced by activin [68]. Evidence suggests that estrogen is synthesized via the following pathway: cholesterol to pregnenolone to androgens to estrogen [23,69,70]. In this study, the *star* was found to be down-regulated, indicating that the upstream processes related to steroid biosynthesis were inhibited. The above analysis demonstrated that genes associated with estrogen synthesis were up-regulated in the hypothalamus. Consequently, MT functions as an exogenous and highly effective androgen in fish, leading to a significant increase in androgen levels within the body. This rise may exert a negative feedback effect on the upstream processes of sex hormone synthesis, thereby inhibiting the conversion of cholesterol to pregnenolone, as well as affecting downstream sex hormone production. Conversely, the positive feedback mechanism enhances the conversion of estrogen. Compared to normal female fish, the estrogen levels may have risen. This finding aligns with the research conducted by Zhu [71], which indicated that the initial expression levels of *P450scc* and *P450arom* in Nile tilapia were down-regulated following MT treatment, subsequently exhibiting an upward trend, with *P450scc* being the first to experience inhibition.

Through KEGG enrichment analysis of liver tissue influenced by MT, we observed significant differences in the expression levels of differential genes, including *cyp1a* and *hsd17b7*. Previous studies have demonstrated that androgen treatment inhibits the expression of cyp1a, which exhibits high catalytic activity for the formation of hydroxyestrogens from estrone (E1) and 17β-estradiol (E2) [53,72]. Additionally, hsd17b7 is an enzyme involved in steroid hormone metabolism that converts E1 into the more potent estrogen E2 [73]. The expression levels of *cyp1a* and *hsd17b7* were up-regulated in this study. This suggested that the concentration of estrogen in liver tissue may increase, thereby enhancing the metabolism of estrogen. These findings align with the analytical results obtained from hypothalamus and gonadal tissues, indicating that the administration of MT compound to feed relatively may promote the conversion of androgens into estrogen.

The results of this study indicate that LZ affects oocyte meiosis and MT influences the synthesis of polyamines in gonadal tissue. This study examines the genetic changes associated with reproduction in golden pompano under the influence of LZ and MT. It provides a fundamental insight into the sex control breeding in the golden pompano.

5. Conclusions

Transcriptome results indicate that in gonadal tissue, LZ promotes the expression of genes associated with the first meiosis of oocytes while simultaneously inhibiting the expression of genes related to the second meiosis. These significant changes impact the trajectory of ovarian differentiation. However, MT enhances the up-regulation of gene expression levels related to the synthesis of polyamines, such as spermidine, but may also induce oocyte apoptosis, thereby influencing the sexual differentiation of female golden pompano. During the process of sex hormone synthesis, LZ inhibits the expression of genes involved in downstream estrogen metabolism but up-regulates the expression of genes associated with upstream cholesterol synthesis, potentially promoting androgen synthesis. In contrast, MT tends to promote the expression of genes associated with estrogen metabolism and repress the expression of genes associated with the conversion of cholesterol to pregnenolone. In conclusion, the present study performs a preliminary exploration of the effects of LZ and MT on the golden pompano before gonadal differentiation, which provides a fundamental insight into the sex control breeding in aquaculture. Future studies could build upon these findings by including a grow-out through the maturation process, with scoring of gross gonadal development and a histological assessment, to further confirm the nature and degree of any sex reversal effects.

Supplementary Materials: The following supporting information can be downloaded at: https://www.mdpi.com/article/10.3390/fishes10010021/s1, Table S1: Primers used in this study; Table S2: Statistics of golden pompano transcriptome sequencing data.

Author Contributions: Conceptualization, H.C.; methodology, Q.Z.; software, Q.Z.; validation, Q.Z., T.W., Y.W., Y.G. and H.C.; resources, Q.Z. and H.C.; data curation, Q.Z.; writing—original draft preparation, Q.Z.; writing—review and editing, Q.Z., T.W. and G.L.; project administration, H.C.; funding acquisition, H.C. All authors have read and agreed to the published version of the manuscript.

Funding: The research leading to these results was financially supported by the Key Research and Development Program of Guangdong (2021B02020200020), the Natural Science Foundation of China (32273131), the Science and Technology Plan of Guangdong Province (2023B0202010016), the Youth Science and Technology Innovation Talent of Guangdong TeZhi plan talent (2023TQ07A888), the Science and Technology Plan of Zhanjiang City (2024E03007), the Science and Technology Plan of Yangjiang City (SDZX2023027 and SDZX2021041), and Research on breeding technology of candidate species for Guangdong modern marine ranching (2024-MRB-00-001).

Institutional Review Board Statement: The experimental protocols for this research were approved by the Animal Research Ethics Committee of Guangdong Ocean University (201903004, approved on 12 March 2019). The study did not involve any endangered or protected species.

Informed Consent Statement: Not applicable.

Data Availability Statement: The raw sequence reads have been submitted to the NCBI database (https://www.ncbi.nlm.nih.gov/bioproject/PRJNA1177985, accessed on 23 October 2024), further inquiries can be directed to the corresponding authors.

Conflicts of Interest: The authors declare no conflicts of interest.

References

1. Martínez, P.; Viñas, A.M.; Sánchez, L.; Díaz, N.; Ribas, L.; Piferrer, F. Genetic architecture of sex determination in fish: Applications to sex ratio control in aquaculture. *Front. Genet.* **2014**, *5*, 340. [CrossRef] [PubMed]
2. Kitano, J.; Ansai, S.; Takehana, Y.; Yamamoto, Y. Diversity and convergence of sex-determination mechanisms in teleost fish. *Annu. Rev. Anim. Biosci.* **2024**, *12*, 233–259. [CrossRef] [PubMed]
3. Mei, J.; Gui, J.F. Genetic basis and biotechnological manipulation of sexual dimorphism and sex determination in fish. *Sci. China Life Sci.* **2015**, *58*, 124–136. [CrossRef] [PubMed]

4. Li, X.Y.; Mei, J.; Ge, C.T.; Liu, X.L.; Gui, J.F. Sex determination mechanisms and sex control approaches in aquaculture animals. *Sci. China Life Sci.* **2022**, *65*, 1091–1122. [CrossRef]
5. Xiong, Y.; Wang, S.; Gui, J.F.; Mei, J. Artificially induced sex-reversal leads to transition from genetic to temperature-dependent sex determination in fish species. *Sci. China Life Sci.* **2020**, *63*, 157–159. [CrossRef]
6. Shen, Z.G.; Fan, Q.X.; Yang, W.; Zhang, Y.L.; Wang, H.P. Effects of 17α-methyltestosterone and aromatase inhibitor letrozole on sex reversal, gonadal structure, and growth in yellow catfish *Pelteobagrus fulvidraco*. *Biol. Bull.* **2015**, *228*, 108–117. [CrossRef]
7. Sun, L.N.; Jiang, X.L.; Xie, Q.P.; Yuan, J.; Huang, B.F.; Tao, W.J.; Zhou, L.Y.; Nagahama, Y.; Wang, D.S. Transdifferentiation of differentiated ovary into functional testis by long-term treatment of aromatase inhibitor in Nile tilapia. *Endocrinology* **2014**, *155*, 1476–1488. [CrossRef]
8. Teng, J.; Zhao, Y.; Chen, H.J.; Xue, L.Y.; Ji, X.S. Global expression response of genes in sex-undifferentiated *Nile tilapia* gonads after exposure to trace letrozole. *Ecotoxicol. Environ. Saf.* **2021**, *217*, 112255. [CrossRef]
9. Karaket, T.; Reungkhajorn, A.; Ponza, P. The optimum dose and period of 17α-methyltestosterone immersion on masculinization of red tilapia (*Oreochromis* spp.). *Aquac. Fish.* **2023**, *8*, 174–179. [CrossRef]
10. Pandian, T.J.; Sheela, S.G. Hormonal induction of sex reversal in fish. *Aquaculture* **1995**, *138*, 1–22. [CrossRef]
11. Guiguen, Y.; Fostier, A.; Piferrer, F.; Chang, C.F. Ovarian aromatase and estrogens: A pivotal role for gonadal sex differentiation and sex change in fish. *Gen. Comp. Endocrinol.* **2010**, *165*, 352–366. [CrossRef] [PubMed]
12. Piferrer, F.; Blázquez, M. Aromatase distribution and regulation in fish. *Fish Physiol. Biochem.* **2005**, *31*, 215–226. [CrossRef] [PubMed]
13. Zhang, F.C.; Tang, C.; Wang, J.Y.; Lin, T.T.; Ge, W.; He, C.Y.; Yang, C.Y.; Zuo, Z.H. Letrozole induced a polycystic ovary syndrome model in zebrafish by interfering with the hypothalamic-pituitary-gonadal axis. *Environ. Pollut.* **2024**, *347*, 123723. [CrossRef] [PubMed]
14. Singh, A.K.; Srivastava, P.P.; Verma, R.; Srivastava, S.C.; Kumar, D.; Ansari, A. Effect of dietary administration of letrozole and tamoxifen on gonadal development, sex differentiation and biochemical changes in common carp (*Cyprinus carpio* L.). *Reprod. Fertil. Dev.* **2015**, *27*, 449. [CrossRef]
15. Zhao, C.; Jiang, M.Y.; Jiang, D.N.; Zhang, J.P.; Hou, X.K.; Zhu, C.H. Induction of premature reversal in plectropomus leopardus by letrozole. *J. Guangdong Ocean Univ.* **2023**, *43*, 19–25. [CrossRef]
16. Kwon, J.Y.; Haghpanah, V.; Kogson-Hurtado, L.M.; McAndrew, B.J.; Penman, D.J. Masculinization of genetic female Nile tilapia (*Oreochromis niloticus*) by dietary administration of an aromatase inhibitor during sexual differentiation. *J. Exp. Zool.* **2000**, *287*, 46–53. [CrossRef]
17. Andriana, D.P.; Thomas, H.U.; Peter, L.G.; Ken, M.B. Effects of 17α-methyltestosterone on uterine morphology and heat shock protein expression are mediated through estrogen and androgen receptors. *J. Steroid Biochem.* **2002**, *82*, 305–314. [CrossRef]
18. Lai, X.J.; Li, Z.Q.; Xie, Y.J.; Chen, S.X.; Wang, Y.L. Androstenedione and 17α-methyltestosterone induce early ovary development of *Anguilla japonica*. *Theriogenology* **2018**, *15*, 16–24. [CrossRef]
19. Xu, D.D.; Yang, F.; Chen, R.Y.; Lou, B.; Zhan, W.; Takao, H.; Yutaka, T. Production of neo-males from gynogenetic yellow drum through 17α-methyltestosterone immersion and subsequent application for the establishment of all-female populations. *Aquaculture* **2018**, *489*, 154–161. [CrossRef]
20. Farias, R.D.S.; Oliveira, K.R.D.S.; Souza, M.E.D.; Ferreira, D.A.; Silva, A.A.D.N.; Silva, V.A.D.; Dunham, R.; Coimbra, M.R.M. Effect of dosage of orally administered 17α-methyltestosterone on sex reversion of the yellowtail tetra *Astyanax lacustris* (Lütken, 1875). *Anim. Reprod.* **2023**, *20*, e20220080. [CrossRef]
21. Liu, S.; Wang, L.; Qin, F.; Zheng, Y.; Li, M.; Zhang, Y.; Yuan, C.; Wang, Z. Gonadal development and transcript profiling of steroidogenic enzymes in response to 17α-methyltestosterone in the rare minnow *Gobiocypris rarus*. *J. Steroid Biochem. Mol. Biol.* **2014**, *143*, 223–232. [CrossRef] [PubMed]
22. Plant, T.M. The hypothalamo-pituitary-gonadal axis. *J. Endocrinol.* **2015**, *226*, T41. [CrossRef] [PubMed]
23. Mathis, G.; Margaret, E.W.; Peter, A.; David, J.H. Reproductive endocrinology of nonalcoholic fatty liver disease. *Endocr. Rev.* **2019**, *40*, 417–446. [CrossRef]
24. Zhang, D.C.; Guo, L.; Guo, H.Y.; Zhu, K.C.; Li, S.Q.; Zhang, Y.; Zhang, N.; Liu, B.S.; Jiang, S.G.; Li, J.T. Chromosome-level genome assembly of golden pompano (*Trachinotus Ovatus*) in the family carangidae. *Sci. Data* **2019**, *6*, 216. [CrossRef]
25. Fan, B.; Xie, D.; Li, Y.; Wang, X.; Qi, X.; Li, S.; Meng, Z.; Chen, X.; Peng, J.; Yang, Y.; et al. A single intronic single nucleotide polymorphism in splicing site of steroidogenic enzyme *hsd17b1* is associated with phenotypic sex in oyster pompano, *Trachinotus anak*. *Proc. Biol. Sci.* **2021**, *288*, 20212245. [CrossRef]
26. Das, D.; Khan, P.P.; Maitra, S. Endocrine and paracrine regulation of meiotic cell cycle progression in teleost oocytes: cAMP at the centre of complex intra-oocyte signalling events. *Gen. Comp. Endocrinol.* **2017**, *241*, 33–40. [CrossRef]
27. Dai, P.; Xiong, L.; Wei, Y.; Wei, X.; Zhou, X.; Zhao, J.; Tang, H. A pancancer analysis of the oncogenic role of cyclin b1 (CCNB1) in human tumors. *Sci. Rep.* **2023**, *13*, 16226. [CrossRef]

28. Ozturk, S. Molecular determinants of the meiotic arrests in mammalian oocytes at different stages of maturation. *Cell Cycle* **2022**, *21*, 547–571. [CrossRef]
29. Cheng, J.; Liu, Y. Knockout of cyclin b1 in granulosa cells causes female subfertility. *Cell Cycle* **2022**, *21*, 1867–1878. [CrossRef]
30. Pei, L. Genomic organization and identification of an enhancer element containing binding sites for multiple proteins in rat pituitary tumor-transforming gene. *J. Biol. Chem.* **1998**, *273*, 5219–5225. [CrossRef]
31. Pei, L. Pituitary tumor-transforming gene protein associates with ribosomal protein S10 and a novel human homologue of DnaJ in testicular cells. *J. Biol. Chem.* **1999**, *274*, 3151–3158. [CrossRef] [PubMed]
32. LaBaer, J.; Garrett, M.D.; Stevenson, L.F.; Slingerland, J.M.; Sandhu, C.; Chou, H.S.; Fattaey, A.; Harlow, E. New functional activities for the P21 family of CDK inhibitors. *Genes Dev.* **1997**, *11*, 847–862. [CrossRef] [PubMed]
33. Broude, E.V.; Demidenko, Z.N.; Vivo, C.; Swift, M.E.; Davis, B.M.; Blagosklonny, M.V.; Roninson, I.B. P21 (CDKN1A) is a negative regulator of p53 stability. *Cell Cycle* **2007**, *6*, 1467–1470. [CrossRef]
34. Miller, J.J.; Summers, M.K.; Hansen, D.V.; Nachury, M.V.; Lehman, N.L.; Loktev, A.; Jackson, P.K. Emi1 stably binds and inhibits the anaphase-promoting complex/cyclosome as a pseudosubstrate inhibitor. *Genes Dev.* **2006**, *20*, 2410–2420. [CrossRef] [PubMed]
35. Reimann, J.D.R.; Freed, E.; Hsu, J.Y.; Kramer, E.R.; Peters, J.M.; Jackson, P.K. Emi1 is a mitotic regulator that interacts with Cdc20 and inhibits the anaphase promoting complex. *Cell* **2001**, *105*, 645–655. [CrossRef]
36. Zhou, C.J.; Wang, X.Y.; Dong, Y.H.; Wang, D.H.; Han, Z.; Zhang, X.J.; Sun, Q.Y.; Carroll, J.; Liang, C.G. CENP-F-dependent DRP1 function regulates APC/C activity during oocyte meiosis I. *Nat. Commun.* **2022**, *13*, 7732. [CrossRef]
37. Verschuren, E.W.; Ban, K.H.; Masek, M.A.; Lehman, N.L.; Jackson, P.K. Loss of emi1-dependent anaphase-promoting complex/cyclosome inhibition deregulates E2F target expression and elicits DNA damage-induced senescence. *Mol. Cell Biol.* **2007**, *27*, 7955–7965. [CrossRef]
38. Marangos, P.; Verschuren, E.W.; Chen, R.; Jackson, P.K.; Carroll, J. Prophase I arrest and progression to metaphase I in mouse oocytes are controlled by Emi1-dependent regulation of APC (Cdh1). *J. Cell Biol.* **2007**, *176*, 65–75. [CrossRef]
39. Baran, V.; Solc, P.; Kovarikova, V.; Rehak, P.; Sutovsky, P. Polo-like kinase 1 is essential for the first mitotic division in the mouse embryo. *Mol. Reprod.* **2013**, *80*, 522–534. [CrossRef]
40. Liu, Z.X.; Sun, Q.R.; Wang, X.S. PLK1, a potential target for cancer therapy. *Transl. Oncol.* **2017**, *10*, 22–32. [CrossRef]
41. Bruno, S.; Ghelli Luserna di Rorà, A.; Napolitano, R.; Soverini, S.; Martinelli, G.; Simonetti, G. CDC20 in and out of mitosis: A prognostic factor and therapeutic target in hematological malignancies. *J. Exp. Clin. Cancer Res.* **2022**, *41*, 159. [CrossRef]
42. Gao, Y.; Guo, C.; Fu, S.; Cheng, Y.; Song, C. Downregulation of CDC20 suppressed cell proliferation, induced apoptosis, triggered cell cycle arrest in osteosarcoma cells, and enhanced chemosensitivity to cisplatin. *Neoplasma* **2021**, *68*, 382–390. [CrossRef] [PubMed]
43. Gui, Y.; Ma, X.; Xiong, M.; Wen, Y.; Cao, C.; Zhang, L.; Wang, X.; Liu, C.; Zhang, H.; Huang, X.; et al. Transcriptome analysis of meiotic and post-meiotic spermatogenic cells reveals the potential hub genes of aging on the decline of male fertility. *Gene* **2024**, *893*, 147883. [CrossRef] [PubMed]
44. Martin, B.T.; Strebhardt, K. Polo-like kinase 1: Target and regulator of transcriptional control. *Cell Cycle* **2006**, *5*, 2881–2885. [CrossRef] [PubMed]
45. Prevo, R.; Pirovano, G.; Puliyadi, R.; Herbert, K.J.; Rodriguez-Berriguete, G.; O'Docherty, A.; Greaves, W.; McKenna, W.G.; Higgins, G.S. CDK1 inhibition sensitizes normal cells to DNA damage in a cell cycle dependent manner. *Cell Cycle* **2018**, *17*, 1513–1523. [CrossRef]
46. Wang, Z.; Fan, M.; Candas, D.; Zhang, T.Q.; Eldridge, A.; Wachsmann-Hogiu, S.; Ahmed, K.M.; Chromy, B.A.; Nantajit, D.; Duru, N.; et al. CyclinB1/Cdk1 coordinates mitochondrial respiration for cell cycle G2/M progression. *Dev. Cell* **2014**, *29*, 217–232. [CrossRef]
47. Pouwels, J.; Kukkonen, A.M.; Lan, W.; Daum, J.R.; Gorbsky, G.J.; Stukenberg, P.T.; Kallio, M.J. Shugoshin 1 plays a central role in kinetochore assembly and is required for kinetochore targeting of Plk1. *Cell Cycle* **2007**, *6*, 1579–1585. [CrossRef]
48. Cicirò, Y.; Ragusa, D.; Sala, A. Expression of the checkpoint kinase BUB1 is a predictor of response to cancer therapies. *Sci. Rep.* **2024**, *14*, 4461. [CrossRef]
49. Fagerberg, L.; Hallström, B.M.; Oksvold, P.; Kampf, C.; Djureinovic, D.; Odeberg, J.; Habuka, M.; Tahmasebpoor, S.; Danielsson, A.; Edlund, K.; et al. Analysis of the human tissue-specific expression by genome-wide integration of transcriptomics and antibody-based proteomics. *Mol. Cell. Proteom.* **2014**, *13*, 397–406. [CrossRef]
50. Ciana, P.; Raviscioni, M.; Mussi, P.; Vegeto, E.; Que, I.; Parker, M.G.; Lowik, C.; Maggi, A. In vivo imaging of transcriptionally active estrogen receptors. *Nat. Med.* **2003**, *9*, 82–86. [CrossRef]
51. Ngee, K.C.; Hudson, W.C.; Andrew, J.B. Squalene monooxygenase: A journey to the heart of cholesterol synthesis. *Prog. Lipid Res.* **2020**, *79*, 101033. [CrossRef]
52. Kullman, S.W.; Hinton, D.E. Identification, characterization, and ontogeny of a second cytochrome P450 3A gene from the fresh water teleost medaka (*Oryzias latipes*). *Mol. Reprod. Dev.* **2001**, *58*, 149–158. [CrossRef] [PubMed]

53. Badawi, A.F.; Cavalieri, E.L.; Rogan, E.G. Role of human cytochrome P450 1A1, 1A2, 1B1, and 3A4 in the 2-, 4-, and 16α-hydroxylation of 17β-estradiol. *Metabolism* **2001**, *50*, 1001–1003. [CrossRef] [PubMed]
54. Lee, A.J.; Cai, M.X.; Thomas, P.E.; Conney, A.H.; Zhu, B.T. Characterization of the oxidative metabolites of 17β-estradiol and estrone formed by 15 selectively expressed human cytochrome P450 isoforms. *Endocrinology* **2003**, *144*, 3382–3398. [CrossRef]
55. Itäaho, K.; Mackenzie, P.I.; Ikushiro, S.; Miners, J.O.; Finel, M. The configuration of the 17-hydroxy group variably influences the glucuronidation of beta-estradiol and epiestradiol by human UDP-glucuronosyltransferases. *Drug Metab. Dispos.* **2008**, *36*, 2307–2315. [CrossRef]
56. Sneitz, N.; Court, M.H.; Zhang, X.; Laajanen, K.; Yee, K.K.; Dalton, P.; Ding, X.; Finel, M. Human UDP-glucuronosyltransferase UGT2A2: cDNA construction, expression, and functional characterization in comparison with UGT2A1 and UGT2A3. *Pharmacogenet. Genom.* **2009**, *19*, 923. [CrossRef]
57. Colciago, A.; Celotti, F.; Pravettoni, A.; Mornati, O.; Martini, L.; Negri-Cesi, P. Dimorphic expression of testosterone metabolizing enzymes in the hypothalamic area of developing rats. *Dev. Brain Res.* **2005**, *155*, 107–116. [CrossRef]
58. Hess, R.A.; Bunick, D.; Lee, K.H.; Bahr, J.; Taylor, J.A.; Korach, K.S.; Lubahn, D.B. A role for oestrogens in the male reproductive system. *Nature* **1997**, *390*, 509–512. [CrossRef]
59. Dostalova, P.; Zatecka, E.; Dvorakova-Hortova, K. Of oestrogens and sperm: A review of the roles of oestrogens and oestrogen receptors in male reproduction. *Int. J. Mol. Sci.* **2017**, *18*, 904. [CrossRef]
60. Su, L.; Yang, K.; Li, S.; Liu, C.; Han, J.; Zhang, Y.; Xu, G. Enolase-phosphatase 1 as a novel potential malignant glioma indicator promotes cell proliferation and migration. *Oncol. Rep.* **2018**, *40*, 2233–2241. [CrossRef]
61. Fontecave, M.; Atta, M.; Mulliez, E. S-Adenosylmethionine: Nothing goes to waste. *Trends Biochem. Sci.* **2004**, *29*, 243–249. [CrossRef] [PubMed]
62. González-Montelongo, M.C.; Marín, R.; Pérez, J.A.; Gómez, T.; Díaz, M. Polyamines transduce the nongenomic, androgen-induced calcium sensitization in intestinal smooth muscle. *Mol. Endocrinol.* **2013**, *27*, 1603–1616. [CrossRef] [PubMed]
63. Bachrach, U. The early history of polyamine research. *Plant Physiol. Biochem.* **2010**, *48*, 490–495. [CrossRef] [PubMed]
64. MacIndoe, J.H.; Turkington, R.W. Hormonal regulation of spermidine formation during spermatogenesis in the rat. *Endocrinology* **1973**, *92*, 595–605. [CrossRef]
65. Murakawa, M.; Jung, S.K.; Iijima, K.; Yonehara, S. Apoptosis-inducing protein, AIP, from parasite-infected fish induces apoptosis in mammalian cells by two different molecular mechanisms. *Cell Death Differ.* **2001**, *8*, 298–307. [CrossRef]
66. Ballatori, N.; Krance, S.M.; Notenboom, S.; Shi, S.; Tieu, K.; Hammond, C.L. Glutathione dysregulation and the etiology and progression of human diseases. *Biol. Chem.* **2009**, *390*, 191–214. [CrossRef]
67. Manna, P.R.; Stetson, C.L.; Slominski, A.T.; Pruitt, K. Role of the steroidogenic acute regulatory protein in health and disease. *Endocrine* **2016**, *51*, 7–21. [CrossRef]
68. Chang, H.M.; Cheng, J.C.; Huang, H.F.; Shi, F.T.; Peter, C.K.L. Activin A, B and AB decrease progesterone production by down-regulating StAR in human granulosa cells. *Mol. Cell. Endocrinol.* **2015**, *412*, 290–301. [CrossRef]
69. Elzenaty, R.N.; Toit, T.D.; Flück, C.E. Basics of androgen synthesis and action. *Best Pract. Res. Clin. Endocrinol. Metab.* **2022**, *36*, 101665. [CrossRef]
70. Taraborrelli, S. Physiology, production and action of progesterone. *Acta Obstet. Gyn. Scand.* **2015**, *94*, 8–16. [CrossRef]
71. Zhu, H.P.; Mo, Y.Y.; Lu, M.X.; Gao, F.Y.; Ye, X.; Huang, Z.H.; Ke, X.L. Effects of 17α-methyltestosterone and letrozole on steroidogenic enzyme gene expression in Nile tilapia (*Oreochromis niloticus*). *J. Fish. China* **2011**, *35*, 1302–1309. Available online: https://kns.cnki.net/kcms2/article/abstract (accessed on 12 October 2024).
72. Monostory, K.; Pascussi, J.M.; Kóbori, L.; Dvorak, Z. Hormonal regulation of cyp1a expression. *Drug Metab. Rev.* **2009**, *41*, 547–572. [CrossRef] [PubMed]
73. Shehu, A.; Mao, J.; Gibori, G.B.; Halperin, J.; Le, J.; Devi, Y.S.; Merrill, B.; Kiyokawa, H.; Gibori, G. Prolactin receptor-associated protein17β-hydroxysteroid dehydrogenase type 7 gene (*hsd17b7*) plays a crucial role in embryonic development and fetal survival. *Mol. Endocrinol.* **2008**, *22*, 2268–2277. [CrossRef] [PubMed]

Disclaimer/Publisher's Note: The statements, opinions and data contained in all publications are solely those of the individual author(s) and contributor(s) and not of MDPI and/or the editor(s). MDPI and/or the editor(s) disclaim responsibility for any injury to people or property resulting from any ideas, methods, instructions or products referred to in the content.